Journal of The
Electrochemical Society

Ecological Recycling of Lithium-Ion Batteries from Electric Vehicles with Focus on Mechanical Processes

To cite this article: Jan Diekmann *et al* 2017 *J. Electrochem. Soc.* **164** A6184

FOCUS ISSUE OF SELECTED PAPERS FROM IMLB 2016 WITH INVITED PAPERS CELEBRATING 25 YEARS OF LITHIUM ION BATTERIES

Ecological Recycling of Lithium-Ion Batteries from Electric Vehicles with Focus on Mechanical Processes

Jan Diekmann,[a,z] Christian Hanisch,[b] Linus Froböse,[a] Gerrit Schälicke,[a] Thomas Loellhoeffel,[a] Anne-Sophie Fölster,[a] and Arno Kwade[a]

[a]*Institute of Particle Technology, TU Braunschweig, 38104 Braunschweig, Lower Saxony, Germany*
[b]*Lion Engineering GmbH, 38106 Braunschweig, Lower Saxony, Germany*

The increasing usage of electrical drive systems and stationary energy storage worldwide lead to a high demand of raw materials for the production of lithium-ion batteries. To prevent further shortage of these crucial materials, ecological and efficient recycling processes of lithium-ion batteries are needed. Nowadays industrial processes are mostly pyrometallurgical and as such energy and cost intensive. The LithoRec projects, funded by the Federal Ministry for the Environment, Nature Conservation, Building and Nuclear Safety (BMUB), aimed at a realization of a new energy-efficient recycling process, abstaining high temperatures and tracing mechanical process-steps. The conducted mechanical processes were thoroughly investigated by experiments in a laboratory and within technical scale, describing gas release of aged and non-aged lithium-ion batteries during dry crushing, intermediates, and products of the mechanical separation. Conclusively, we found that applying a second crushing step increases the yield of the coating materials, but also enables more selective separation. This work identifies the need for recycling of lithium-ion batteries and its challenges and hazard potential in regards to the applied materials. The outlined results show a safe and ecological recycling process with a material recycling rate of at least 75%.

Manuscript submitted September 30, 2016; revised manuscript received November 11, 2016. Published December 7, 2016. This was Paper 75 presented at the Chicago, Illinois, Meeting of the IMLB, June 19–24, 2016. *This paper is part of the Focus Issue of Selected Papers from IMLB 2016 with Invited Papers Celebrating 25 Years of Lithium Ion Batteries.*

The growing demand of lithium-ion batteries (LIB) for electric or hybrid electric vehicles, as well as the increasing usage of portable electronic devices and stationary energy storage systems[1,2] lead to an ever increasing request of raw materials needed for their production. In order to satisfy this demand while conserving natural resources and decreasing costs for raw materials, an ecologically friendly and efficient recycling process is needed. Additionally, such a recycling process minimizes growing disposal as well as non-qualified handling.

Resources.—The composition of a generic battery system of an electric vehicle (EV) based on an analysis of different systems and estimations of experts[3] is shown in Figure 1. The system periphery mainly consists of an aluminum (Al) casing, but also contains the battery management unit (BMU) and cables. While the periphery of the battery modules is made of similar components, they mostly contain only small slave BMUs. The displayed data show, that around 55 wt% of a battery system are dedicated to the battery cells containing the electrolyte (here volatile components), separator (plastics), cell housing (Al), and the electrodes. While the anode is a copper (Cu) foil mainly coated with graphite, the main component of the cathode coating is a transition metal oxide which, in this case, is lithium nickel cobalt manganese oxide ($LiNi_{0,33}Co_{0,33}Mn_{0,33}O_2$). The contents of an EV battery system with average weight consists of 3.5 kg of lithium (Li), 10.9 kg of nickel (Ni), 10.9 kg of cobalt (Co), and 9.8 kg of manganese (Mn). These high quantities emphasize the necessity for recycling of these materials.

Nowadays recycling processes focus on the recovery of the most valuable materials Ni and Co.[4–6] Next to the high commodity prices for these materials, Delucchi et al.[7] expect future shortage due to the increasing production of lithium-ion batteries. The worldwide cobalt resources will be insufficient in less than 60 years for the production of 20 million EV battery systems per year. Additionally, the demand of nickel for the same amount of battery systems will be considerably larger than current worldwide extraction.[7] Although the raw material costs of lithium (Li) are lower than those of Ni and Co, its future recovery is seen as crucial by some researchers. Gruber et al.[8] estimate high lithium resources, but also point out that the element has to be recycled with a recycling rate around 90% to prevent future shortage. Vikström et al.[9] calculated that even the most optimistic production scenario will not attain the estimation for lithium demand made by the International Energy Agency of around 100 kt in 2030.[10] In contrast, researchers of the TRU Group Inc.[11] evaluated a massive lithium oversupply trough 2020 by using a model that predict a lithium supply twice as big as its demand due to pipeline projects and capacity expansions.

However, next to the worldwide resources, local natural deposits are playing an important role. The most profitable lithium sources are located in areas like China and South America. Consequently, recycling will represent the most important supply of lithium for countries without or less direct resources in the next centuries.[12]

Additionally, there will be significant amounts of spent lithium-ion batteries in the next years,[4,13] as it is also strongly connected to e-waste recycling.[14–16] To avoid their disposal and enable ecologically friendly recycling, new processes have to be developed.

Unit operations and industrial processes for the recycling of LIB.—Recycling processes for LIB are a combination of different unit operations: Deactivation, pyrometallurgical, mechanical, and hydrometallurgical treatment.

Deactivation can be carried out by discharge of the whole battery system, battery modules, or battery cells. To avoid relaxation behavior,[17,18] namely the rise of voltage after discharge of the batteries, short-circuiting is required. Another deactivation method consists of a thermal pre-treatment. During this process the batteries are heated up to maximum temperatures around 300°C. At this temperature gas generation and evaporation of the solvents take place, which opens the battery cells, combusts the electrolyte solvents, and therefore inactivates the batteries.[19,20] Although a disassembly of the battery systems does not deactivate them, it lowers the attached energy by decreasing the size. Normally, all further processing steps require a disassembly process.

Preparation of the regained battery modules, cells, or coating materials can be carried out pyrometallurgically or mechanically afterwards. Utilizing pyrometallurgical treatment leads to recovery of Ni, Co, and Cu in the molten mass.[20]

[z]E-mail: j.diekmann@tu-braunschweig.de

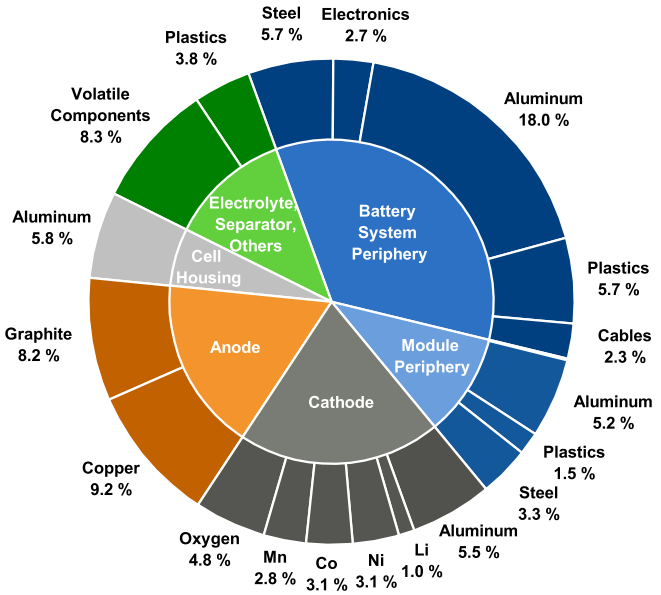

Figure 1. Generic composition of EV battery system.

Mechanical treatment combines crushing, classification, and sorting processes. Most studies use mechanical processes to expose the high valuable coating materials for further investigation of hydrometallurgical and pyrometallurgical processes,[21–23] or even spouted bed elutriation.[24] Furthermore, a large number of these were carried out with laboratory equipment and battery cells from consumer devices or laptops, which are normally different to automotive battery cells. Wang et al.[25] proposed a pre-recycling process for discharged lithium-ion batteries with several sieving treatments. This simple process enables the concentration of the different metal composites in fractions and is easy scalable. The here presented work takes a step forward to an achievable and scalable mechanical preparation route for battery modules of electric vehicles.

Special procedures are combinations of thermal and mechanical processes using temperatures above 400°C which decompose the state of the art binder polyvinylidene fluoride (PVDF) resulting in lower adhesion between current collector foil and coating.[25,26] The following mechanical treatment enables recovery of the coating materials with very high purity.[27]

Hydrometallurgical treatment is applied for the direct recovery of metals, such as Co, Ni, Mn, and Li, from the mechanical separated coating materials[28,29] as well as for the extraction of Al and Li from slag of pyrometallurgical processes.[20] To achieve this, leaching and several preparation processes are employed. Also mechanochemical approaches can be found in the literature.[30]

As mentioned before, a combination of different recycling unit operations is needed. To show the variety of the recycling processes, two exemplary processes are briefly described in the following. More detailed descriptions of different industrial processes can be found in literature.[19,27,31,32]

The Canadian enterprise Retriev (former Toxco Inc.) uses a combination of mechanical and hydrometallurgical treatments. Crushing of the sorted spent battery cells is carried out by a hammer mill under brine solution. This wet crushing leads to decreased reactivity of the battery cells and avoids harmful emissions. The resulting fragments undergo a mechanical separation process to regain Al, Cu, and Co in a subsequent process. Additionally, Co and a Li brine can be retrieved from the remaining fluids.[19]

A combination of pyrometallurgical and hydrometallurgical processes is used by the Belgian Umicore group. The so called Val'Eas process starts with a three sectional furnace. A preheating treatment deactivates the batteries by evaporation of the electrolyte solvents. The following pyrolysis melts the plastic components at a temperature of 700°C before alloy and slag matter are regained at temperatures of up to 1450°C. As the alloy contains Co, Cu, Ni, and iron (Fe) the slag consists of Li, Al, silicon (Si), and calcium (Ca). Afterwards, the alloy is treated hydrometallurgical to recover refined Co and Ni compounds.[19]

The mentioned processes have distinct disadvantages such as high energy input for pyrometallurgical treatment, the lack of Li recovery, high output of liquid hazardous waste for wet crushing, and low material recycling rates. Therefore, the LithoRec projects focused on the development of a mainly mechanical recycling process followed by a hydrometallurgical treatment of the coating materials.

Challenges in recycling of LIB from EV or HEV.—Challenges in the recycling of lithium-ion batteries begin with the battery cells themselves. The high diversity of applied materials regarding electrolyte composition and the electrode coating chemistries enhance the design of processes handling these components. A particular challenge for the hydrometallurgical processing of the regained coating powders are the variations in its chemistry or purity, but ongoing development is promising here.[6] Next to the chemical deviation, different cell formats (e.g. cylindrical or prismatic/ hard case or pouch) and cell housing materials influence the design of battery modules and systems. Every cell and module manufacturer, as well as every automobile manufacturer applies its own design. Especially the high diversity of battery system architectures regarding housing, but also electrical contacts and BMU concepts complicates automatic process of discharge and disassembly. As battery modules are mostly feed material for a first crushing, the crusher has to be designed for different module sizes and housing materials. The main challenge for mechanical preparation procedures is the separation of current collector foils and electrochemical active coating materials, as electrodes of lithium-ion batteries are made for long lasting adhesion. To achieve a high yield of pure materials, a combination of different processes is needed.

One of the main challenges in the recycling of lithium-ion batteries is their hazard potential. Due to health and safety, as well as environment protection, these hazards have to be taken into account for process design, transportation, and storage.

The hazard potential of lithium-ion batteries can be divided into three areas: electrical hazard, fire and explosion hazard, and chemical hazard. The electrical hazard is determined by the stored electric energy and high voltage. A battery system emits a direct current, which can cause pyrolysis of the blood due to an electric shock. Short circuits of lithium-ion batteries lead to elevated temperatures as a result of joule heating. The contemporary applied carbonates of the electrolyte (e.g. dimethyl carbonate and ethyl methyl carbonate) are flammable and contribute to the fire and explosion hazard. The highly flammable reaction products, like methane, ethane, and propene can cause fire and explosions. The chemical hazard could be induced by toxic gaseous reaction products like carbon monoxide (CO) and hydrogen fluoride (HF) resulting from the decomposition of the state of the art conducting salt lithium hexafluorophosphate ($LiPF_6$) and the binder PVDF. Furthermore, the partly carcinogenic cathode active materials (nickel and cobalt oxides) have to be considered as chemical hazard. Next to these critical substances organic fluorophosphates generated from ageing are highly toxic.[33]

The mentioned three areas are interacting: a short circuit could lead to elevated temperatures and exothermal reactions, or even a thermal runaway in the worst case scenario. During these exothermal reactions toxic and flammable gases are released, potentially ending in fire and/or explosion. There are several good overviews about the hazard potential of lithium-ion batteries.[34–36]

As mentioned before, the conducting salt $LiPF_6$ decomposes at high temperatures. Furthermore, this decomposition is influenced by humidity.[37–40] Through the contact with aerial humidity $LiPF_6$ generates HF and other products like organic fluorophosphates and nitric acid. This can be observed in the crushing product of loaded lithium-ion battery cells. After crushing "micro-short-circuits" between anode and cathode fragments increase the local temperature of the crushing product. The high local temperatures cause $LiPF_6$ to decompose at

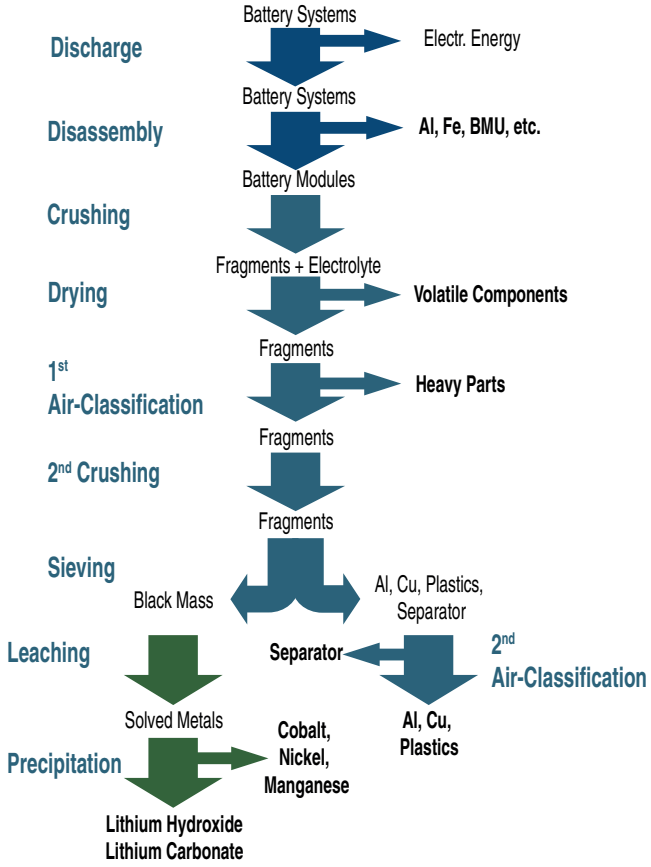

Figure 2. LithoRec process chain.

around 60°C and in contact with aerial humidity which leads to a release of HF and other toxic gaseous products.

Generally, nearly every recycling process has to deal with economic challenges. Therefore, it is important to find a balance between the required purity of recycling products, the usage of energy, and the investment in the process equipment.

The LithoRec Process.—The LithoRec process combines electrical, mechanical, mild thermal, and hydrometallurgical treatment with the aim of recovering nearly all valuable materials of battery systems.[28,41] An overall process flow chart is shown in Figure 2. A more detailed depiction of the mechanical process steps is presented in Figure 3.

The battery system gets discharged and short circuited to lower the electrical hazard, regain the remaining energy, and enable safe disassembly and crushing. The short circuit avoids relaxation and inherent voltage rise of the battery and plays a role during the following disassembly of the battery system. Due to the many design deviations an automation of this process is not suitable, but short circuiting of every module protects the disassembler. The above mentioned challenges in the disassembly to battery modules produce a large number of necessary steps.[42] The removed battery system peripheries such as the tray, housing, cables, BMU, is fed to established recycling routes. Automation such as human-robot collaboration reduce costs and increase disassembly efficiency.[43]

Afterwards, the dismantled battery modules are crushed. Because of the flammable electrolyte components this process is conducted under inert atmosphere while the released gases are cleaned by activated carbon.

The following drying step aims to remove the remaining components of the electrolyte. At temperatures of around 100 to 140°C and decreased pressure the organic solvents of the electrolyte are being vaporized. Nowadays, electrolyte solvents are mixtures of linear carbonates like dimethyl (DMC), ethyl methyl (EMC), or diethyl carbonate (DEC), and cyclic carbonates like propylene (PC), or ethylene carbonate (EC). The vaporized solvents can be recovered by condensation or combusted via a thermal post-combustion process which regains the thermal energy. Additionally, the conducting salt $LiPF_6$ is decomposed while generating HF as a gaseous product. HF leads to the necessity of a gas scrubber application. The removal of the electrolyte components leads to an improved separation process due to a lower adhesion between the crushing fragments and a minimized hazard potential of intermediates and products (no HF generation, no inherent flammable solvents).

The following mechanical separation is a combination of air-sifting, crushing and sieving processes. A possible combination and enclosed process influences will be described later on. One product of the mechanical separation is the coating of anode and cathode, the so called black mass. The process route from discharging of whole battery systems to classification and sieving processes was realized in a demonstration plant within technical scale.

As mentioned before the black mass contains the transition metal oxide lithium nickel cobalt manganese oxide (NCM) and graphite. This powder is processed hydrometallurgically to recover the metals. At first, the recovered fraction is leached and solid graphite is removed. Metals like Ni, Co, or Mn are precipitated via pH manipulation and a precursor is prepared. The remaining Li solution is cleaned by several process steps. After crystallization lithium hydroxide or lithium carbonate is produced. The combination of lithium hydroxide or lithium carbonate and the precursor can be used for new battery active material.[44] Two aspects or the hydrometallurgical recovery of metals from the black mass of spent lithium-ion batteries have to be considered. Firstly, the black mass has to be unmixed which means lithium iron phosphate (LFP) cannot be processed together with NCM due to different precipitation limits. And secondly, the contamination have to be taken into account as, especially high impurities from the carbonates, Cu, and Al will have a negative effect on the purity of the resynthesized battery active material.[44]

This manuscript focuses on the mechanical exposure and separation processes. As the gas release during the first crushing is playing a major role for the process design, differently aged batteries were crushed in laboratory scale. The main content of this work is the description of the influences of a second crushing step on the yield of black mass and the separation of materials, as well as investigating intermediates and products in regards to their composition. These experiments were carried out with field tested battery modules in technical scale.

Experimental

Figure 3 shows the developed process chain. The investigated process steps are crushing (Gas release during crushing) and the separation processes of the first air-classification, second crushing, sieving, and second air-classification (Mechanical separation).

Gas release during crushing.—The experiments regarding gas release of LIB during crushing were carried out using Panasonic CGR18650CH 18650 battery cells with a nominal voltage of 3.6 V and capacity of 2250 mAh. The amount of volatile components of the cells were determined via manual disassembly and drying at 75°C until no further weight loss was examined. The cells were single crushed via a six-disk-rotor in a converted cutting mill. For crushing within a nitrogen atmosphere the cutting mill was surrounded with a stainless steel housing with gas feed and exhaust. The gas measurement was implemented via Online-Fourier Transform Infrared Spectroscopy (FTIR).

The experiments were performed using fourfold determination. To determine the influence of State of Health (SOH) on gas release, four battery cells were cycled to 80% SOH with a C-rate of 1 C. All cells were unloaded (1/10 C) to 1 V and short-circuited for at least 24 hours afterwards. The discontinuous crushing process is explained in

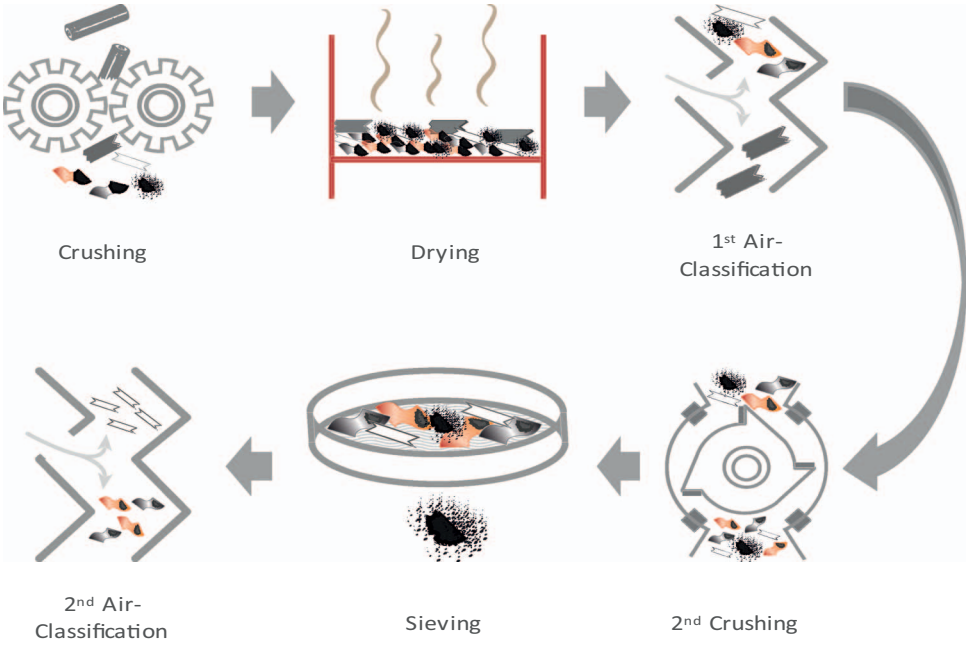

Figure 3. Process steps of the investigated recycling process with varied 2nd crushing.

Figure 4. Inert rendering was carried out with a higher volume flow of N_2 (13 l min^{-1}) until the concentration of carbon dioxide (CO_2) was below 30 ppm and humidity below 0.4 vol.-%. This CO_2 concentration is equal to 1.65 vol.-% of oxygen. During crushing the volume flow of N_2 corresponds to the volume flow of the FTIR of 4 l min^{-1}. The atmosphere in the cutting mill housing was purged after the crushing procedure.

Mechanical separation.—The experiments for the investigation of process influences on yield and separation efficiency were carried out with field tested EV battery modules with an average weight of 4.95 kg. These modules contain six prismatic 25 Ah battery cells with NCM and graphite as cathode and anode active materials. Mass balances of module housing and battery cells were triple determined via manual disassembly, drying and weighing of the different materials. Area densities of the coated and uncoated electrodes were used to calculate the masses of coating materials. The used battery modules were regained from discharged, short-circuited, and disassembled battery systems.

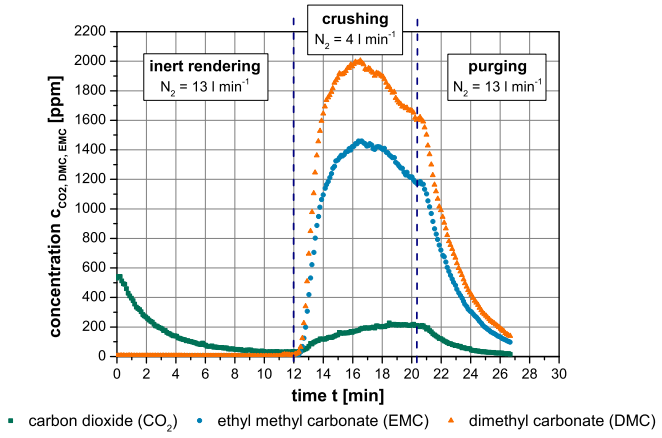

Figure 4. Different phases of a discontinuous crushing process.

The battery modules were crushed via a rotary-shear with four shafts and a 20 mm discharge screen under nitrogen atmosphere with an oxygen concentration of 4 vol.-%. The incurred module fragments were dried at a temperature of 105°C for five hours and then mixed. Composition of the intermediate was determined by sieving analysis and manual sorting. Density determination was carried out via optical area, thickness, and weight measurement. Particle size and density were used for the calculation of a separating parameter for air-classification processes. This separating parameter is commonly used for the estimation of the selectivity of zig-zag-sifting processes and combines the crucial factors of a separation via air classification: particle size regarding face area and therefore uplift force, as well as density. Similar separating values have a negative influence on the selectivity of the separation. Calculation of the separating parameter is shown in Equation 1.

$$separating\ parameter = x \cdot \sqrt{\rho} \qquad [1]$$

where x = particle size [mm], ρ = density [g cm^{-3}].

The first mechanical separation treatment, the first air-classification, recovers the heavy parts, such as casing materials from module and cells, electric conductors, and steel screws. For different dense materials with same particle sizes, zig-zag-sifting enables a separation via density by a cascade of cross-flow sifting. While materials with a smaller density are located in the light product, materials with higher density are found in the heavy product. This classification was carried out with a mass load μ_s of 190 g kg^{-1} air and an air velocity v_s of 3.34 m s^{-1}. The products' composition was determined by manual sorting. To show the influence of a second crushing on yield and separation efficiency this process was added as comparison, using a cutting mill with a 10 mm discharge screen. A vibration sieve with a mesh size of 500 µm was used in order to separate the black mass from the current collector foils and the separator. The determination of the black mass' components and its impurities of Cu, Al, and Fe were carried out via ICP-OES. At least a second air-classification via a zig-zag-sifter removes the valueless separator from the current collector foil fragments. The separation of the separator was carried out with different air velocities v_s and a mass load μ_S of 25 g kg^{-1} air. Mass output and therefore the separation efficiency was also ascertained by manual sorting which requires a lot of time. Therefore, the reproducibility of product compositions of the sifting and sieving

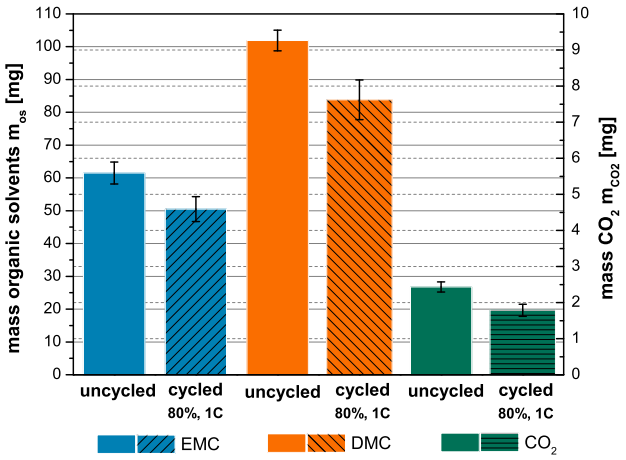

Figure 5. Masses of the released gases ethyl methyl carbonate (EMC), dimethyl carbonate (DMC), and carbon dioxide (CO_2) during crushing.

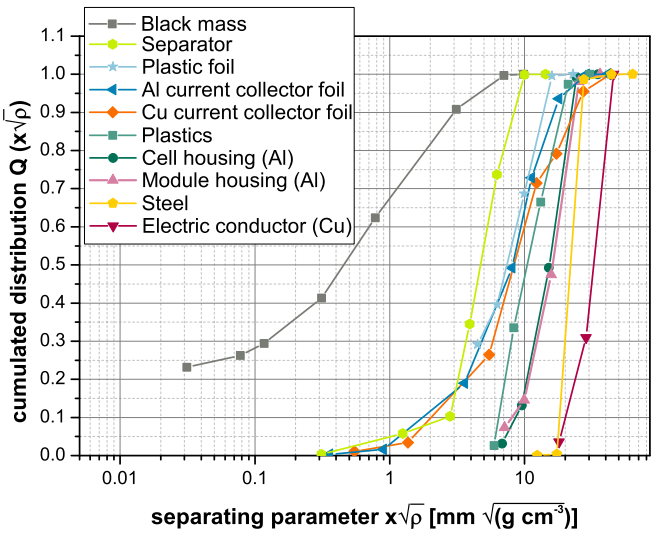

Figure 6. Cumulated distribution of different materials of a crushed and dried battery module.

processes were determined with single battery cells (25 Ah) for one process route and parameter set-up as a triple determination.

Results and Discussion

Influence of SOH on gas release during crushing.—The first crushing procedure transfers the battery modules into conveyable and storable bulk material. Valuable materials of the battery as well as gaseous components are released during this process step. As shown in Figure 4 the electrolyte solvents DMC and EMC, as well as carbon dioxide (CO_2) are the main infrared active components of the atmosphere in the cutting mill housing. The highest concentration of DMC is around 2000 ppm (0.2 vol.-%) which is far away from its lower explosion limit of 4.22 vol.-%. Similarly, the concentrations of EMC are not within critical range. CO_2 is a known gaseous reaction intermediate during cycling and therefore aging of LIB.[33,45–47]

Regarding the released masses of the gaseous products (Figure 5) a difference between the aged and non-aged battery cells become more obvious. The released mass of all gas species is lower for cycled battery cells than for the non-cycled. DMC and EMC are reduced during onward ageing, as their reaction with Li form components of the solid electrolyte interface (SEI), such as CH_3OCO_2Li. Evolution of this layer during prolonged cycling is regarded to be the main source of anode ageing according to many researchers.[48–50]

As mentioned before CO_2 is an ageing product. Therefore, the cycled battery cells were expected to give rise to higher amounts of CO_2 during crushing. However, prolonged cycling can lead to a reduction of CO_2 as it is proposed that $ROCO_2Li$ can undergo a reduction with traces of water and CO_2 which can form lithium carbonate ($LiCO_3$) as a solid ageing product.[48,50–52]

The overall gas release of cycled cells is 18% smaller than for uncycled, simply formatted cells. During crushing of 18650 battery cells of this type only 3.6 wt% and respectively 4.5 wt% of the overall volatile components (8.8 wt% of battery cell mass) were released as the gaseous components DMC, EMC, and CO_2. FTIR measurements of the atmosphere in the inner space of a technical scale crusher show that the lower explosion limit of DMC is reached by crushing only three kilograms of 25 Ah battery cells for the used crusher type.[41]

Influences on the separation processes.—During crushing and drying the mass of the module fragment is reduced by the amount of its volatile components (in this case 8.05 wt%). The mass loss is dedicated to the evaporation of the electrolyte solvents and the decomposition of $LiPF_6$.

Input material for the mechanical separation.—A sieving analysis, manual sorting, and density calculation of the different materials of the crushed and dried battery module lead to a cumulated distribution connected with the separating parameter as shown in Figure 6. As mentioned above, similar separating parameters have a negative influence on the selectivity of the separation. The analyzed fragments consist of all applied materials of the battery module. Regarding the separating parameter, separation of battery cell current collector foils Al (4.7 wt%) and Cu (8.4 wt%) from separator (3.4 wt%) and plastic foils would unselective, especially for smaller fragment sizes. The use of the separating parameter also indicates that a separation of the battery module components with higher densities, such as module housing (9.6 wt%), cell housing (17.2 wt%), plastics (2.3 wt%), and steel (4.9 wt%) from the remainder is possible via zig-zag-sifting.

The black mass (48.7 wt%), containing anode and cathode coating, is present in agglomerate sizes from 20 µm to fragment sizes up to 6.3 mm. Fragments under 20 µm are mostly primary NCM particles with an average size of 10 µm. Under these crushing and drying conditions hardly any coating remains on the current collector foils. This can be explained by the generation of HF and the subsequent loss of adhesion by leaching oxide layers between current collector foil and coating.

1st air-classification.—As mentioned above, components with higher densities are recovered via a first air-classification. The light product of the sifting process consists of the current collector foils, black mass, separator, and plastic foils. The recovered heavy parts include 74.3 wt% Al from module and cell housing, 13.8 wt% Fe, 5.0 wt% Cu, and 4.0 wt% plastics. Additionally, these fraction contains 2.9 wt% of inclusions. These inclusions are compounds of current collector foils, separator, and black mass and present a first loss for the yield on Cu, Al, and black mass. Although this loss occurs, removal of the heavy parts is essential to protect the cutting tools of a potential second crushing process. The change in the overall cumulated distribution of the particle sizes after the first air-classification can be seen in Figure 8.

Influence of 2nd crushing on the black mass yield.—To show the influence of a second crushing on process and product, one process route without and another with a second crushing are compared in the following. A cutting mill with a discharge screen of 10 mm was used for a "mild" crushing. The cutting mill itself mainly exerts a cutting stress on the fragments but also increases an overall mechanical stress.

The yield of black mass with and without application of a second crushing is shown in Figure 7. The second crushing increases the yield of black mass from 60% to 75%. This increase occurs due to comminution of the black mass fragments as well as the decomposition of the previously mentioned inclusions. Comparing the cumulated distributions after 1st classification and after 1st classification/2nd crushing

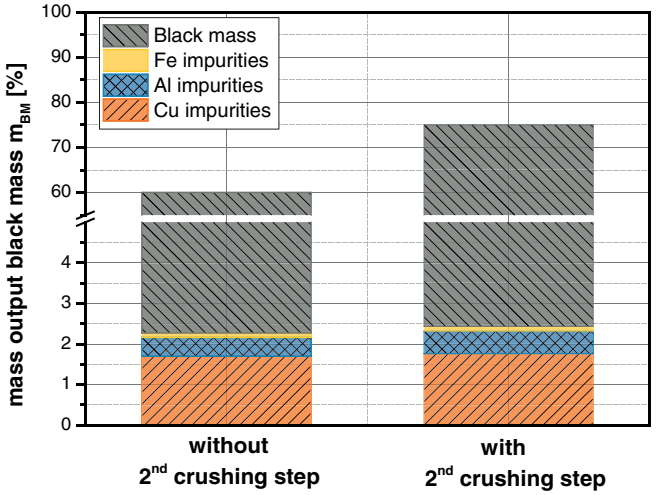

Figure 7. Yield of the black mass and impurities with/ without 2nd crushing step.

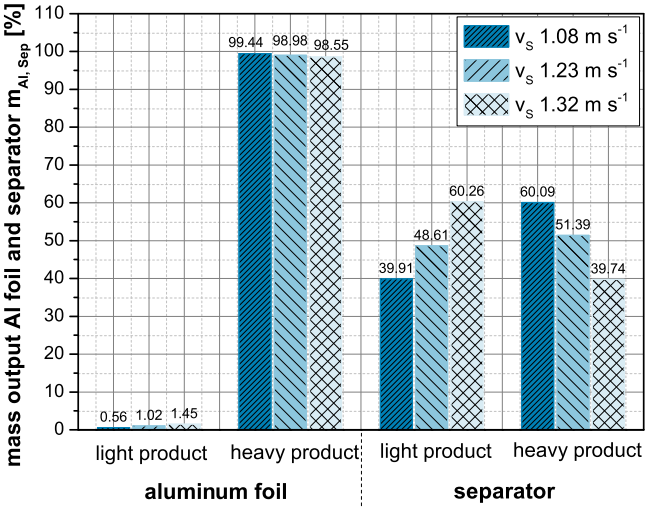

Figure 9. Mass output of separator and aluminum in light and heavy product of the 2nd air-classification without 2nd crushing step.

in Figure 8, an increased mass of the fraction smaller 200 and 500 µm can be observed. This change in the fraction mass leads to a significant higher yield through sieving at 500 µm. Importantly, the second crushing hardly increases the impurities from the current collector foils Cu and Al. Cu impurities are increased from 1.7 to 1.8 wt% and the concentration of Al rises from 0.5 to 0.6 wt%. This small change is due to the "mild" crushing and mainly cutting stress induced by the cutting mill. As no change in Fe concentration (0.1 wt%) is measured, this contamination is not induced by the second crushing. Following hydrometallurgical processing of the regained coating materials removes these impurities by precipitation or ion exchange. Furthermore, Krüger et al.[44] investigated that low Al impurities have no negative effect on the electrochemical performance of resynthesized cathode active material.

Influence of 2nd crushing on the 2nd air-classification.—An additional crushing step also influences the second air-classification via zig-zag-sifting. This process step is necessary to remove the valueless separator, which is mainly poly ethylene nowadays, from the valuable materials of the current collector foils. The main aim of this process step is the removal of separator from the heavy product with simultaneously small loss of aluminum foil located in the light product, as this fraction will be disposed.

Figure 9 shows the amount of the overall aluminum and separator located in the heavy and light product of the sifting process for three different air velocities without preceding a second crushing. In general, an increase of the air velocity leads to a smaller mass output of the separator in the heavy product, and a higher mass output of aluminum in the light product. A classification without previous further crushing is not precise. For an acceptable loss of aluminum foil of 1.02 wt%, 51.39 wt% of the separator contaminates the heavy product. The high share of the separator in the heavy product results from inclusions of separator, current collector foils, and black mass as well as the great amount of higher fragment sizes of the separator fragments (Figure 6 and Figure 8).

The influence of a further crushing is outlined in Figure 10, showing the share of aluminum and separator in heavy and light product of the second classification with a preceded second crushing. For a loss of aluminum foil in the light product of 0.9 wt%, the share of separator in the heavy product can be reduced to 23.7 wt% at an air velocity v_s of 1.1 m s^{-1}. The data also show that the separation can be carried out more selectively. The reasons for higher selectivity of the sifting process after a second crushing can be found in the cumulated

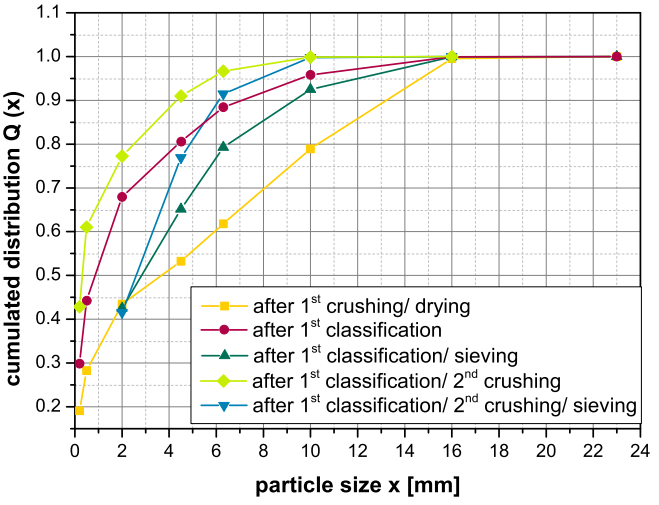

Figure 8. Change of the cumulated distribution of fragments of a battery module after different process steps. The cumulated distributions relate to the light product after classification and to the residue after sieving.

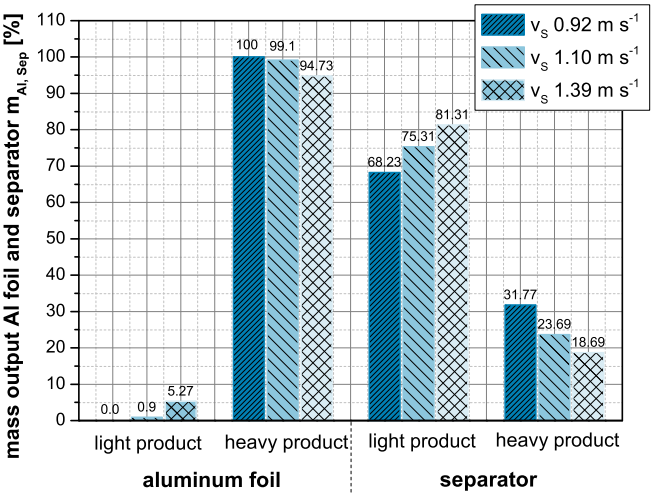

Figure 10. Mass output of separator and aluminum in light and heavy product of the 2nd air-classification with preceding 2nd crushing step.

Table I. Compositions of heavy and light product after 2nd classification (μ_s 25 g kg^{-1}, v_s 1.1 m s^{-1}).

Component	Composition heavy product (wt%)	Composition light product (wt%)
Al-foil	16.6	1.6
Cu-foil	29.8	-
separator	2.9	97.8
plastics	5.9	0.6
black mass	44.8	-

distribution of particle or fragment sizes as seen in Figure 8. Further crushing limits the upper fragment size to <16 mm and decomposes the mentioned inclusions. The following sieving additionally limits the lower particle size to >500 µm. These factors lead to a more homogenous intermediate regarding fragment sizes. For a closer particle size distribution, the materials densities are becoming more important for the selectivity of air-classification which lead to a more precise separation. The products of the selected process route (with second crushing) and parameters are shown in Table I. In a significant way, the remaining black mass has a high share in the composition of the foil fraction. Further processing of this fraction enables a retrieval of remaining black mass. Intensive air-sieving, where the fragments are accelerated by an air flow, can recover about 41 wt% of the remaining black mass, leading to an overall yield of 85%. The fragments are stressed by an impact leading to decomposition of black mass fragments and therefore a higher yield <500 µm.

Hanisch et al.[27] presented a process with a coupling of incineration and air sieving. In their work they decomposed the binder to lower the cohesion between particles, as well as adhesion between the particles and the current collector foil. The following air-sieving recovers the black mass via impact stress. The application of this process to the foil fraction from the recycling process achieves 67 wt% mass output of the remaining black mass <500 µm. The incineration process has to be carried out under oxygen atmosphere to additionally incinerate the plastics in the foil fraction. This provokes high Cu corrosion, leading to higher Cu impurities in the black mass during air sieving.

Reproducibility of the mechanical separation processes.—To show the reproducibility of the data from sieving and sifting processes a triple determination of a process route was carried out. The standard deviation of compositions of the sieving yield and sifting product is shown in Figure 11. As the single battery cells were the same type as previously investigated battery modules no influence of other housing, separator material, current collector foils materials, binder, electrolyte, or coating material is expectable. The relatively higher deviation for black mass in the light product of the second classification can be explained by its very low amount. Overall this data confirms the reproducibility of the investigated sieving and air-classification processes. It has to be taken into account that manual sorting leads to an average loss of 2.4 wt% of the total mass.

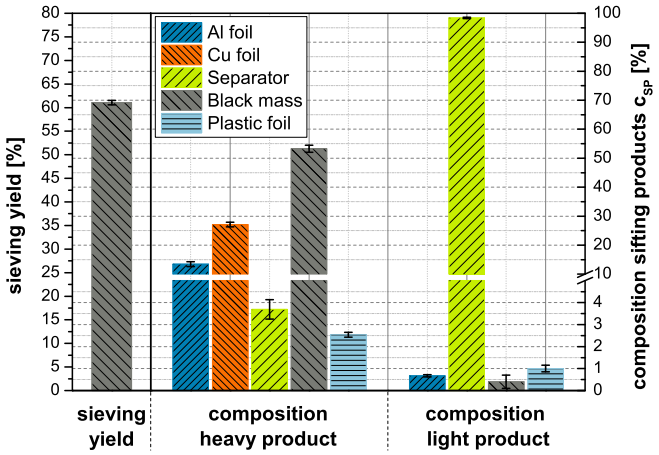

Figure 11. Standard deviation of a triple determination of the sieving yield and the composition of the zig-zag-sifting products.

Conclusions

The increasing amount of electric and hybrid electric vehicles leads to a need for an ecological and economic recycling of lithium-ion batteries in following years. Recovery of components like copper, aluminum, nickel, cobalt, manganese, and lithium of spent batteries will be crucial, especially for countries with less or no raw material reserves. Main challenges for a recycling process are purity of the recycling products, efficiency during their production, and a safe process design.

This work presents a functional, safe, and efficient process for the recycling of lithium-ion battery systems from electric and hybrid electric vehicles. The use of predominantly mechanical processes leads to an ecological process design with a positive impact on the global warming potential.[3]

Mechanical processes during recycling of lithium-ion batteries are characterized by different focus areas. During crushing of battery cells or modules the release of flammable gas components plays a major role. The released gas species depend on the electrolyte components like the applied solvents, but also on gaseous ageing products. The overall gas release of DMC, EMC, and CO_2 of the investigated batteries at a SOH of 80% during crushing is significantly smaller than the gas release of simply formatted cells, due to ageing reactions. For crushing battery modules from EV the usage of an inert atmosphere remains with no alternative. After the removal of electrolyte components by drying, separation of the different materials is the main goal. A "mild" second crushing step via a cutting mill increases the yield of black mass to 75%. Most importantly, this process step only leads to a small increase of copper and aluminum impurities. The recovered black mass contains 1.8 wt% copper, 0.6 wt% aluminum, and 0.1 wt% iron. Additionally, this process leads to a better removal of the valueless separator via air-classification. Further crushing limits the upper fragment size and decomposes inclusions, resulting in a homogenized particle size distribution.

Overall products of the presented process are housing materials and electronics recovered during disassembly, heavy part components of the battery modules from first air-classification, black mass from sieving, and a foil fraction from a second classification. These products lead to an overall material recycling rate of 75%, not including separator, electrolyte, and graphite from the anode coating as those are non-recyclable fractions nowadays. However, in the future a direct recycling of active material particles out of spent graphite or NCM might be possible.

Acknowledgments

The authors thank the German Federal Ministry for the Environment, Nature Conservation, Building and Nuclear Safety for the funding of research projects LithoRec I (Reference No. 16EM0023) and LithoRec II (Reference No. 16EM1024). Furthermore, thank you to all project partners in LithoRec I and LithoRec II, especially Dr. Steffen Sander, Matthias Petermann, and Guido Sellin. The authors also thank Uwe Stüwe, Ernst Jelting, Detlev Hille, Ulrike Lau, and the Institute of Energy and Process Systems Engineering for the collaboration. Special thanks got to Dr. Randolph Schließer and Anke Bösel from the VDI/ VDE-IT for the support.

References

1. G. P. Hammond and T. Hazeldine, *Applied Energy*, **138**, 559 (2015).
2. B. Scrosati and J. Garche, *Journal of Power Sources*, **195**(9), 2419 (2010).

3. M. Buchert and J. Sutter, (Ö.-I. e.V., ed.), p. 85. Öko-Institut e.V., Berlin, Darmstadt, 2015.
4. C. Hoyer, K. Kieckhäfer, and T. S. Spengler, *Journal of Business Economics*, **85**(5), 505 (2014).
5. S. Ziemann, M. Weil, and L. Schebek, *Resources, Conservation and Recycling*, **63**, 26 (2012).
6. J. Heelan, E. Gratz, Z. Zheng, Q. Wang, M. Chen, D. Apelian, and Y. Wang, *Jom*, **68**(10), 2632 (2016).
7. M. A. Delucchi, C. Yang, A. F. Burke, J. M. Ogden, K. Kurani, J. Kessler, and D. Sperling, *Philosophical transactions. Series A, Mathematical, physical, and engineering sciences*, **372**(2006), 20120325 (2014).
8. P. W. Gruber, P. A. Medina, G. A. Keoleian, S. E. Kesler, M. P. Everson, and T. J. Wallington, *Journal of Industrial Ecology*, **15**(5), 760 (2011).
9. H. Vikström, S. Davidsson, and M. Höök, *Applied Energy*, **110**, 252 (2013).
10. IEA, *International Energy Agency*, 52 (2011).
11. E. R. Anderson, *in* "3rd Lithium Supply & Markets Conference", Vol. 2016, Toronto, 2011.
12. J. H. Miedema and H. C. Moll, *Resources Policy*, **38**(2), 204 (2013).
13. S. Ziemann, A. Grunwald, L. Schebek, D. B. Müller, and M. Weil, *Revue de Métallurgie*, **110**(1), 47 (2013).
14. M. Kaya, *Waste Manag*, **57**, 64 (2016).
15. X. Zeng, Q. Song, J. Li, W. Yuan, H. Duan, and L. Liu, *Journal of Cleaner Production*, **90**, 55 (2015).
16. X. Zeng, J. Li, and L. Liu, *Renewable and Sustainable Energy Reviews*, **52**, 1759 (2015).
17. D. M. Bernardi and J.-Y. Go, *Journal of Power Sources*, **196**(1), 412 (2011).
18. M. A. Roscher, O. Bohlen, and J. Vetter, *International Journal of Electrochemistry*, **2011**1 (2011).
19. A. Vezzini, 529 (2014).
20. T. Georgi-Maschler, B. Friedrich, R. Weyhe, H. Heegn, and M. Rutz, *Journal of Power Sources*, **207**, 173 (2012).
21. F. Pagnanelli, E. Moscardini, P. Altimari, T. Abo Atia, and L. Toro, *Waste Manag*, **51**, 214 (2016).
22. S. M. Shin, N. H. Kim, J. S. Sohn, D. H. Yang, and Y. H. Kim, *Hydrometallurgy*, **79**(3-4), 172 (2005).
23. E. Gratz, Q. Sa, D. Apelian, and Y. Wang, *Journal of Power Sources*, **262**, 255 (2014).
24. D. A. Bertuol, C. Toniasso, B. M. Jiménez, L. Meili, G. L. Dotto, E. H. Tanabe, and M. L. Aguiar, *Journal of Power Sources*, **275**, 627 (2015).
25. J. Li, R. Zhao, X. He, and H. Liu, *Ionics*, **15**(1), 111 (2008).
26. L. Sun and K. Qiu, *Journal of hazardous materials*, **194**, 378 (2011).
27. C. Hanisch, T. Loellhoeffel, J. Diekmann, K. J. Markley, W. Haselrieder, and A. Kwade, *Journal of Cleaner Production*, **108**, 301 (2015).
28. C. Hanisch, J. Diekmann, A. Stieger, W. Haselrieder, and A. Kwade, in *Handbook of Clean Energy Systems*, J. Yan, ed., Wiley UK (2015).
29. X. Zeng, J. Li, and B. Shen, *Journal of hazardous materials*, **295**, 112 (2015).
30. M. M. Wang, C. C. Zhang, and F. S. Zhang, *Waste Manag*, **51**, 239 (2016).
31. C. O. Vadenbo, *in* "Institute for Environmental Decisions", p. 176, Zürich, 2009.
32. X. Zeng, J. Li, and N. Singh, *Critical Reviews in Environmental Science and Technology*, **44**(10), 1129 (2014).
33. C. L. Campion, W. Li, and B. L. Lucht, *Journal of The Electrochemical Society*, **152**(12), A2327 (2005).
34. J. Wen, Y. Yu, and C. Chen, *Materials Express*, **2**(3), 197 (2012).
35. R. Spotnitz and J. Franklin, *Journal of Power Sources*, **113**, 19 (2002).
36. C. Mikolajczak, K. Kahn, K. White, and R. T. Long, The Fire Protection Research Foundation, Quincy, Massachussetts, 2011.
37. L. Terborg, S. Nowak, S. Passerini, M. Winter, U. Karst, P. R. Haddad, and P. N. Nesterenko, *Analytica chimica acta*, **714**, 121 (2012).
38. V. Kraft, M. Grutzke, W. Weber, M. Winter, and S. Nowak, *Journal of chromatography. A*, **1354**, 92 (2014).
39. K. Xu, *Chemical reviews*, **114**(23), 11503 (2014).
40. S. Wilken, P. Johansson, and P. Jacobsson, *Solid State Ionics*, **225**, 608 (2012).
41. J. Diekmann, C. Hanisch, T. Loellhoeffel, G. Schälicke, and A. Kwade, *ECS Transactions - The Electrochemical Society*, **73**, 9 (2016).
42. C. Herrmann, A. Raatz, M. Mennenga, J. Schmitt, and S. Andrew, *in* "19th CIRP International Conference on Life Cycle Engineering", Berkeley, 2012.
43. C. Herrmann, A. Raatz, S. Andrew, and J. Schmitt, *Advanced Materials Research*, **907**, 391 (2014).
44. S. Krüger, C. Hanisch, A. Kwade, M. Winter, and S. Nowak, *Journal of Electroanalytical Chemistry*, **726**, 91 (2014).
45. S. E. Sloop, J. K. Pugh, S. Wang, J. B. Kerr, and K. Kinoshita, *Electrochemical and Solid-State Letters*, **4**(4), A42 (2001).
46. S. E. Sloop, J. B. Kerr, and K. Kinoshita, *Journal of Power Sources*, **119–121**, 330 (2003).
47. G. Gachot, P. Ribière, D. Mathiron, S. Grugeon, M. Armand, J.-B. Leriche, S. Pilard, and S. Laruelle, *Anal. Chem.*, **83**, 478 (2011).
48. J. Vetter, P. Novák, M. R. Wagner, C. Veit, K. C. Möller, J. O. Besenhard, M. Winter, M. Wohlfahrt-Mehrens, C. Vogler, and A. Hammouche, *Journal of Power Sources*, **147** (1), 269 (2005).
49. D. Aurbach, E. Zinigrad, Y. Cohen, and H. Teller, *Solid State Ionics*, **148**, 11 (2002).
50. C. Lin, A. Tang, H. Mu, W. Wang, and C. Wang, *Journal of Chemistry*, **2015**, 1 (2015).
51. P. Röder, B. Stiaszny, J. C. Ziegler, N. Baba, P. Lagaly, and H.-D. Wiemhöfer, *Journal of Power Sources*, **268**, 315 (2014).
52. M. Lu, H. Cheng, and Y. Yang, *Electrochimica Acta*, **53**(9), 3539 (2008).